Available online at www.sciencedirect.com
SCIENCE DIRECT®
Journal of Magnetic Resonance 159 (2002) 87–91
JMR Journal of Magnetic Resonance
www.academicpress.com

A new contrast parameter for visualization of the cross-link density in rubber based on the dipolar-correlation effect

F. Grinberg,[a,*] M. Heidenreich,[a,1] and W. Kuhn[b]

[a] *Sektion Kernresonanzspektroskopie, Albert-Einstein-Allee 11, Universität Ulm, 89069 Ulm, Germany*
[b] *IIC Innovative Imaging Corp. KG, Langental 18, D-66440 Blieskastel, Germany*

Received 8 February 2002; revised 29 July 2002

Abstract

A new parameter for NMR mapping is suggested on the basis of the mean squared dipolar fluctuation (MSDF). The MSDF characterizes the relaxation mechanism due to ultra-slow dipolar fluctuations in liquids subject to local anisotropy of molecular motions. These fluctuations can be monitored on the time scale exceeding a few microseconds. In rubber materials, the MSDF is a function of the density of chemical cross-links strongly affecting (anisotropic) mesh chain fluctuations. Experimentally, the MSDF is determined from the attenuation curves of the quotient of the amplitudes of the stimulated and the primary echoes produced by the three 90° radio-frequency pulse sequence. In order to evaluate the MSDF maps, the latter sequence was combined with the standard scheme of the magnetic field gradients providing a spatial resolution. The pixel values of the MSDF are "visualized" using grey shades related to the equidistant intervals covering the whole range of the measured values. The MSDF maps are demonstrated for the two composite samples. The first sample consists of a water filled tube in the middle part surrounded by high molecular mass polyisoprene (PI) in the outer part. The relaxation weighted spin density image of this sample is dominated by a water signal with PI producing a much weaker intensity. The MSDF map, on the contrary, enhances the relative intensity of the outer, PI, part while scaling the middle, water, part down to the level of noise. The second sample consists of the four rubber pieces with different cross-link density. This sample thus models an inhomogeneous rubber object. The MSDF map produces clear contrast for the relevant regions. The advantages of employing this kind of NMR mapping for a characterization of materials are discussed.

Keywords: Rubber; Cross-link density; The dipolar-correlation effect; NMR imaging; Mean squared dipolar fluctuation

1. Introduction

A parameter selective NMR mapping has well established itself as a useful tool of a material characterization [1–6]. In our recent papers [7–9], we demonstrated that rubber materials with the different cross-link density can be distinguished on the basis of the so-called dipolar-correlation effect (DCE). The DCE defines the relaxation mechanism caused by ultraslow fluctuations of the (residual) dipolar couplings in anisotropic liquids. The time scale of the fluctuations addressed by the DCE is that of the inter-pulse spacings in the standard $90°$–τ_1–$90°$–τ_2–$90°$ pulse sequence ($10^{-5} < t < 10$ s in the case of protons). The upper limit is ultimately determined by spin-lattice relaxation and represents the longest time scale generally accessible to NMR techniques. In rubber materials, the relevant dipolar fluctuations are caused by slow reorientations of the long-chain backbones around the local symmetry axis. The latter is determined by the mean positions of permanent chemical cross-links (and/or other topological constraints) restricting isotropic molecular reorientations on the time scale of the NMR experiment.

The quantitative analysis of the DCE is based on the measurements of the quotient of the amplitudes of the primary, $A_{\mathrm{pr}}(2\tau_1)$, and the stimulated, $A_{\mathrm{st}}(2\tau_1 + \tau_2)$, echoes as a function of τ_1. (The magnetic field inhomogeneities are supposed to be small, so that the attenuation due to translational molecular diffusion is

* Corresponding author. Fax: +731-502-3150.
E-mail address: farida.grinberg@physik.uni-ulm.de (F. Grinberg).
[1] Present address: Bruker BioSpin MRI, D-76275 Ettlingen, Germany.

1090-7807/02/$ - see front matter © 2002 Elsevier Science (USA). All rights reserved.
PII: S1090-7807(02)00007-1

excluded.) The quotient $Q_{dc} = A_{st}/A_{pr}$ is formed in order to eliminate the parts of the overall transverse relaxation arising from the fluctuations of the dipolar coupling constant fast on the time scale of the inter-pulse intervals. The (local intrachain) molecular motions with typical correlation times much shorter than the time scale addressed by the DCE do not contribute to the attenuation of $Q_{dc}(\tau_1)$ as a function of τ_1. This statement is valid under the assumption that the underlying ultraslow and fast stochastic molecular motions are statistically (quasi)-independent of each other. In this case, the respective parts of the transverse relaxation can be factorized. The attenuation due to the fast motions (usually evaluated in terms of the relaxation time, T_2) is equal for both the primary and the stimulated echo amplitudes and cancels in the quotient. Note that in absence of the slow dipolar fluctuations (in isotropic non-viscous liquids, for instance) the quotient of the both amplitudes becomes independent of τ_1.

If the quotient, $Q_{dc}(\tau_1)$, attenuates with τ_1, this appears to be indicative for the long-time scale orientational dipolar fluctuations. The most clear manifestation for an attenuation by the DCE mechanism was observed in a nematic liquid crystal [10]. In the isotropic state, the experimentally measured quotient $Q_{dc}(\tau_1)$, was found to be constant as expected for any ordinary liquids. At the same time, a strong decrease of Q_{dc} with τ_1 was observed for the temperatures below the clearing point. The attenuation mechanism in the latter case was identified with the contributions of ultraslow collective molecular motions characteristic of liquid crystals in the nematic state. The DCE was also reported for linear polymers [11,12], polymeric liquid crystals [13] and rubber materials [7–9] as mentioned above.

The attenuation of the dipolar-correlation quotient, $Q_{dc}(\tau_1)$, is quantitatively described in terms of the mean squared dipolar fluctuation (MSDF) of the residual dipolar coupling constant, $\Omega_d(t)$, and the time constants characteristic of (dipolar) correlation losses on the time scale of the inter-pulse intervals. For macroscopically disordered systems like unstretched polymers or rubbers, the dipolar-correlation quotient is given in the form [8]

$$Q_{dc} = \exp\left\{ -\frac{1}{4}\langle \delta\Omega_d^2 \rangle C_1 \right\}, \tag{1}$$

where

$$\delta\Omega_d(t) \equiv \Omega_d(t) - \langle \Omega_d \rangle. \tag{2}$$

Here, Ω_d denotes the part of the dipolar constant remaining after averaging over fast molecular motions, that is

$$\Omega_d = \Omega_0 \langle (1 - 3\cos^2 \alpha_{kl}) \rangle, \tag{3}$$

where $\Omega_0 = 3\mu_0\gamma^2\hbar/(8\pi r_{kl}^3)$, r_{kl} and α_{kl} are polar coordinates of the inter-nuclear vector, the brackets indicate the average on the time scale $t \ll \tau_1, \tau_2$. (If local anisotropy of the system persists on much longer time scale, this average is not zero). $\delta\Omega_d(t)$ in Eq. (2) stands for the part of the "residual" dipolar constant, Ω_d, fluctuating around its mean value, $\langle \Omega_d \rangle$, on the (much longer) time scale of the pulse intervals, τ_1, τ_2. Such slow modulations of Ω_d may, for instance, easily arise due to the small-angle reorientations of the end-to-end vector, **R**, connecting the two adjacent cross-links (or other constraints). For an exponential correlation function $\langle \delta\Omega_d(0)\delta\Omega_d(t) \rangle \propto \exp -|t|/\tau_c$ with the correlation time τ_c, the coefficient C_1 in Eq. (1) is [10]:

$$C_1 = \tau_c^2 \left(e^{-\tau_1/\tau_c} - 1 \right)^2 \left(1 - e^{-\tau_2/\tau_c} \right) \tag{4}$$

In rubber, Ω_d is determined by the angle θ formed by the vector **R** relative to the magnetic field [14–16]

$$\Omega_d \approx \Omega_0 \frac{R^2}{N^2 b^2} (1 - 3\cos^2\theta), \quad |\mathbf{R}| = R \ll Nb, \tag{5}$$

where N is the number of statistical segments of length b in the chain mesh spanned by **R**.

The dependence of the MSDF, $\langle \delta\Omega_d^2 \rangle$, on N was estimated [9] in the limit of $R \ll Nb$ using Eqs. (5) and (2)

$$\begin{aligned} \langle \delta\Omega_d^2 \rangle &\equiv \langle (\Omega_d(t) - \langle \Omega_d \rangle)^2 \rangle \\ &\approx \Omega_0^2 \frac{R^4}{(N^2 b^2)^2} \left\langle \left[\left(1 - 3\cos^2\theta\right) - \langle 1 - 3\cos^2\theta \rangle \right]^2 \right\rangle, \\ &R \ll Nb. \end{aligned} \tag{6}$$

Hence, $\langle \delta\Omega_d^2 \rangle$ is the parameter strongly depending on the density, N^{-1}, of the constraints. Strong sensitivity of $\langle \delta\Omega_d^2 \rangle$ to the density of chemical cross-links was experimentally proven in the (bulk) DCE experiments for a series of cross-linked synthetic poly-(styrene-butadiene) [9] elastomers and natural rubber [8]. The aim of the present paper is to demonstrate a combination of the DCE with the methods of spatial resolution in order to produce spatially resolved maps of the MSDF as a new parameter for characterization of (inhomogeneous) polymer materials.

2. Experimental

NMR experiments were performed with a commercial Bruker DSX400 operating at 400 MHz for protons. A standard bore microimaging probe with a 10 mm radio-frequency coil was used.

Materials of natural rubber (NR) based on polyisoprene (PI) with different cross-link density were provided by Bundesanstalt für Materialforschung und-prüfung, Berlin, Germany. The amounts of sulfur, P_s, used for the vulcanization of the rubber samples were equal to 1.0 (NR-E1), 1.5 (NR-E2), 2.0 (NR-E3), and 2.5 (NR-E4) phr (parts per hundred rubber [17]). The cross-link density defined as the inverse of the number of segments

$\tilde{N}$ between the nearest neighbour cross-links is proportional to P_s [17], that is, $\tilde{N}^{-1} = \alpha P_s$ where α is the coefficient depending on a technological procedure and vulcanizing agents used. Here, $\tilde{N}$ identifies the number of segments between the chemical cross-links only. It should therefore be differentiated from N in Eq. (5) which refers to the number of chain segments between the two adjacent topological constraints of *any origin* as long as they maintain their mean positions in space on the time scale of the inter-pulse spacings, see [7] for more detail. Some additional characteristics of the investigated rubber samples like maximal swelling levels can be found in the same work [7]. Linear *cis*-polyisoprene (PI) with an average molecular weight of 8×10^5 g/mol was obtained from Sigma–Aldrich (Steinheim aA).

The pulse sequence used for the MSDF mapping is shown in Fig. 1. It combines the radio-frequency pulse sequence for measurements of the primary and stimulated echo amplitudes with the standard scheme of the magnetic field gradients necessary for a spatial resolution (see, for instance [1,12] or other text books for NMR imaging). The first 90°-pulse of the sequence might either be "hard" (if no slice selection is required) or "soft" (shaped) suited for slice selection purposes. In the case of the relaxation weighted spin density (RWSD) images in Figs. 2a and 3a and the MSDF maps in Figs. 2b and 3b, the first 90°-pulse was "hard" and the gradient pulse in the direction of the Zeeman field, G_z, was not applied. By omitting any slice selection, advantage was taken of the cylindrical symmetry of the investigated samples in order to reduce the time necessary for signal accumulations. The in-plane pixel resolution of the 128×128 data matrixes in Figs. 2 and 3 was 78 μm in both directions. Field of view was 10 mm. The measurements have been performed using the chemical-shift

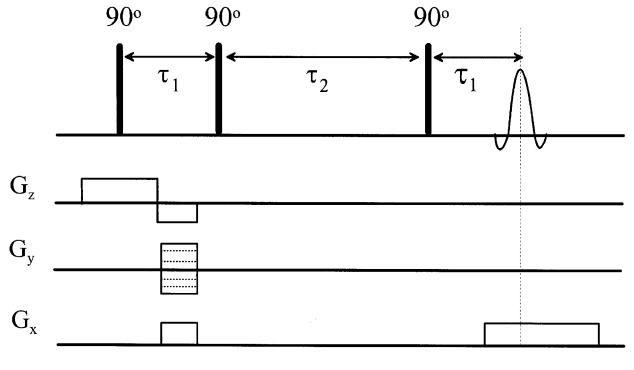

Fig. 1. Pulse sequence for measuring the MSDF maps. G_x, G_y, and G_z denote the pulses of magnetic field gradients in X-, Y-, and Z-directions with Zeeman field applied along the Z-axis as usual. Signal amplitudes are acquired for the stimulated and primary echoes subject to maximal refocusing at $2\tau_1 + \tau_2$ and $2\tau_1$, respectively. In the case of the primary echo, τ_2 is set to zero and the third 90° pulse is omitted. The chemical-shift compensating version of the pulse sequence includes two additional 180°-pulses set in the middle of each τ_1-interval, that is, between the first two 90°-pulses and between the echo time and the preceding pulse.

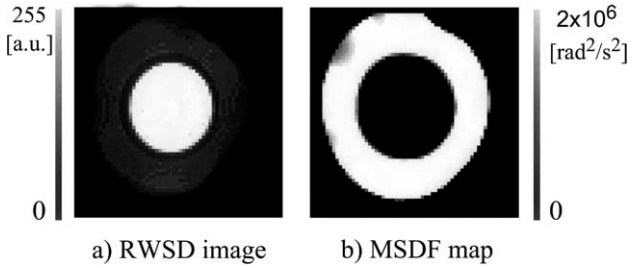

Fig. 2. RWSD image (a) and the MSDF map (b) of the sample consisting of a water filled glass tube (interior part) and PI (outer part). The RWSD image in (a) refers to the primary echo for $\tau_1 = 0.9$ ms (echo time $2\tau_1 = 1.8$ ms). Each data matrix consists of 128×128 pixels. The in-plane pixel resolution is 78 μm in both directions. Field of view is 10 mm. The repetition time was 1 s. The range of the values measured for (a) the RWSD from 0 to 255 arbitrary units and for (b) $\langle \delta\Omega_d^2 \rangle$ from 0 to 2×10^6 rad^2/s^2 is displayed using the grey shade reference rulers shown on the left and on the right hand sides. The ruler assigns consistently decreasing grey shades (from black to white) to each of the 255 subsequent equidistant intervals covering the whole range of the measured values.

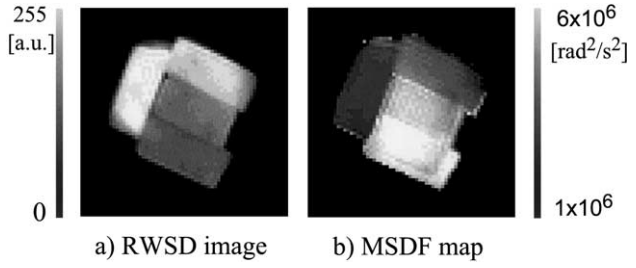

Fig. 3. RWSD image (a) and the MSDF map (b) of the sample consisting of four rubber stripes with different cross-link density. The RWSD image in (a) refers to the primary echo for $\tau_1 = 0.9$ ms (echo time $2\tau_1 = 1.8$ ms). Each data matrix consists of 128×128 pixels. The in-plane pixel resolution is 78 μm in both directions. Field of view is 10 mm. The repetition time was 1 s. The range of the values measured for (a) the RWSD from 0 to 255 arbitrary units and for (b) $\langle \delta\Omega_d^2 \rangle$ from 1×10^6 to 5×10^6 rad^2/s^2 is displayed using the grey shade reference rulers shown on the left and on the right hand sides. The ruler assigns consistently decreasing grey shades (from black to white) to each of the 255 subsequent equidistant intervals covering the whole range of the measured values.

compensating version [8,9] of the pulse sequence shown in Fig. 1. It includes two additional 180°-pulses set in the middle of each τ_1-interval, that is, between the first two 90°-pulses and between the echo time and the preceding pulse. The additional 180°-pulses ensure the absence of amplitude distortions due to cross-relaxation between chemically in-equivalent environments.

The primary and stimulated echo signals were acquired for a series of 32 subsequently increasing τ_1-values. The shortest value of τ_1 in the series was equal to 0.9 ms. The value of τ_2 was kept constant equal to 20 ms. The repetition time, that is, the interval between any two successive exitations by the first 90°-pulse, was 1 s. For each given value of τ_1 echo signals were averaged using

32 scans. The amount of time needed was about 70 min. The total time spent for acquisition of 32 primary and 32 stimulated echo signals was about 75 h. The dipolar-correlation quotients were formed for each pixel of the given map to produce sets of values, $Q_{dc}(\tau_1)$. The values of $\langle \delta\Omega_d^2 \rangle$ were evaluated for the individual pixels by fitting Eqs. (1) and (4) to the obtained data sets. These values were then "visualized" in the grey shade MSDF maps. The grey shade maps were produced by subdividing the overall range of the measured values of $\langle \delta\Omega_d^2 \rangle$ in 255 equidistant intervals. Each interval was assigned a certain grey shade intensity identified in the reference rulers in Figs. 2 and 3. The individual pixels of the maps were then displayed with the grey shades of those intervals to which the pixel values of $\langle \delta\Omega_d^2 \rangle$ were matching to. The grey shade RWSD images shown in Figs. 2a and 3a refer to the primary echo for the shortest value of $\tau_1 = 0.9$ ms in the series (that is, echo time $2\tau_1$ was 1.8 ms). The RWSD images visualize the measured pixel signal intensity proportional to spin density attenuated by transverse relaxation. The attenuation mechanism in this case is due to both fast and slow stochastic molecular fluctuations. Grey shades are produced in the same manner as for the MSDF maps.

3. Results and discussion

Fig. 2 shows the RWSD image (a) and the MSDF map (b) of the same composite sample consisting of two parts. The interior part of the sample is a thin glass tube filled with water. The outer part is linear PI. The RWSD image in Fig. 2a is dominated by a water signal (white middle) whereas the signal from PI (grey outer part) is scaled down by faster (compared to water) transverse relaxation. The black ring separating the signals from water and PI is produced by the inner glass tube. Its signal cannot be discriminated from a noise level which is "black." In contrast to the RWSD image, the MSDF map in Fig. 2b now shows the water part "black." This is due to the absence of the long time-scale dipolar correlations in such an isotropic non-viscous liquid like water. In this case, the primary and the stimulated echo attenuate with increasing τ_1 at the same rate. The quotient of the both amplitudes then becomes independent of τ_1, so that the values of $\langle \delta\Omega_d^2 \rangle$ fitted to experimental data are ≈ 0. The area related to water in the MSDF map thus is scaled down to a noise level and cannot be distinguished from the inner glass tube. The outer, PI's, area in the MSDF map on the contrary occurs "white" pointing out the strong attenuation mechanism due to the DCE [7]. Note that in the RWSD image, the PI's area can only slightly be distinguished from the noise even for the relatively short $\tau_1 = 0.9$ s (compare, for instance, grey shades in the outer part and in the adjacent black ring produced by the inner glass tube).

Figs. 3a and b represent the RWSD image (a) and the MSDF map (b) of the composite rubber sample, respectively. This sample consists of the four stripes (NR-E1, NR-E2, NR-E3, and NR-E4) of rubber with different cross-link density. The composite sample models an inhomogeneous rubber material. The values of $\langle \delta\Omega_d^2 \rangle$ evaluated for the corresponding areas of the map satisfactorily coincide with those found earlier for NR-E1—NR-E4 in the bulk measurements [8]. The regions with larger cross-link density (lower molecular mobility) are brighter according to their larger values of $\langle \delta\Omega_d^2 \rangle$, consider Eq. (6).

Contrast in the RWSD image in Fig. 3a is obviously produced by the difference in the transverse relaxation rates in the individual rubber stripes, assuming that their initial magnetizations (proportional to spin density) are roughly equal. By the echo time, the corresponding magnetizations are attenuated stronger for the stripes with larger cross-link density resulting in darker regions. Contrast in the RWSD images thus depends on the experimental parameters used (echo time in this case) as in any relaxation attenuated spin density image. The (single parameter) MSDF maps, on the contrary, enable one to visualize the areas with different orientational molecular mobility on the quantitative basis.

The map parameter $\langle \delta\Omega_d^2 \rangle$ generally characterizes the part of the transverse relaxation caused by long-time scale dipolar correlations. In studies of materials, the areas with reduced orientational mobility of molecules are quite often of a special interest. They may, for instance, indicate the aging processes in polymer elastomers. On the basis of the MSDF maps, the areas less mobile are favourably scaled up relative to the more mobile ones. An additional advantage in the context of material characterization is that the attenuation mechanism due to the DCE is expected to be insensitive to the traces of low-molecular impurities or to the motions like reorientations of the short free-end chains.

Worth noting is that in systems subject to slow correlated molecular motions, the overall transverse relaxation is generally not exponential [8–10]. Therefore, the conventional transverse-relaxation time (T_2) maps cannot be properly evaluated, as routinely done, on the basis of the Hahn echo attenuation curves. Mapping of the MSDF offers in such cases an alternative quantitative tool for the investigations of the heterogeneous objects exposed to ultraslow dipolar correlations.

Acknowledgments

We like to express our special thanks to Prof. Dr. R. Kimmich, in whose excellent laboratory and with whose closest support and stimulating discussions this research has been performed. We further thank Prof. N. Chandrakumar for a valuable help in course of the ex-

periments. F.G. acknowledges the financial support by the Ministerium für Wissenschaft, Forschung und Kunst Baden-Württemberg and by the Deutsche Forschungsgemeinschaft.

References

[1] B. Blümich, NMR Imaging of Materials, Oxford, Clarendon Press, 2000.
[2] P. Blümler, B. Blümich, R. Botto, E. Fukushima (Eds.), Spatially Resolved Magnetic Resonance. Methods, Materials, Medicine, Biology, Rheology, Geology, Ecology, Hardware, Wiley/VCH, Weinheim, New York, Chichester, Brisbane, Singapore, Toronto, 1998.
[3] B. Blümich, W. Kuhn (Eds.), Magnetic Resonance Microscopy. Methods and Application in Materials Science, Agriculture, and Biomedicine, VCH, Weinheim, New York, Basel, Cambridge, 1992.
[4] W. Kuhn, P. Barth, P. Denner, R. Müller, Characterisation of elastomeric materials by NMR-microscopy, Solid State Nucl. Magn. Reson. 6 (1996) 295–308.
[5] M. Knorgen, K.F. Arndt, S. Richter, D. Kuckling, H. Schneider, Investigation of swelling and diffusion in polymers by ^{1}NMR imaging: LCP networks and hydrogels, J. Mol. Struct. 554 (2000) 69–79.
[6] H. Kühn, M. Klein, A. Wiesmath, D.E. Demco, B. Blümich, J. Kelm, P.W. Gold, The NMR-MOUSE(R): quality control of elastomers, Magn. Reson. Imaging 19 (2001) 497–499.
[7] M. Garbarczyk, F. Grinberg, N. Nestle, W. Kuhn, A novel NMR approach to the determination of the cross-link density in rubber materials with the dipolar correlation effect in low magnetic fields, J. Polym. Sci. B 39 (2001) 2207–2216.
[8] F. Grinberg, M. Garbarczyk, W. Kuhn, Influence of the cross-link density and the filler content on segment dynamics of dry and swollen natural rubber studied by the NMR dipolar-correlation effect, J. Chem. Phys. 111 (1999) 11222–11231.
[9] E. Fischer, F. Grinberg, R. Kimmich, S. Hafner, Characterisation of polymer networks using the dipolar correlation effect on the stimulated echo and field-cycling nuclear-magnetic resonance relaxometry, J. Chem. Phys. 109 (1998) 846–854.
[10] F. Grinberg, R. Kimmich, Characterisation of order fluctuations in liquid crystals by the dipolar-correlation effect on the stimulated echo, J. Chem. Phys. 103 (1995) 365–370.
[11] R. Kimmich, E. Fischer, P. Callaghan, N. Fatkullin, The dipolar-correlation effect on the stimulated echo. Application to polymer melts, J. Magn. Reson. A 117 (1995) 53–61.
[12] R. Kimmich, NMR: Tomography, Diffusometry, Relaxometry, Springer, Heidelberg, 1997.
[13] F. Grinberg, R. Kimmich, M. Möller, A. Molenberg, Order fluctuations in the mesophase of polydiethylsiloxane as studied by the dipolar-correlation effect on the stimulated echo, J. Chem. Phys. 105 (1996) 9657–9665.
[14] P. Sotta, C. Fülber, D.E. Demco, B. Blümich, H.W. Spiess, Effect of residual dipolar interactions on the NMR relaxation in cross-linked elastomers, Macromolecules 29 (1996) 6222–6230.
[15] J.-P. Cohen-Addad, Effect of the anisotropic chain motion in molten polymers: The solid-like contribution of the nonzero average dipolar coupling to NMR signals. Theoretical description, J. Chem. Phys. 60 (1974) 2440–2453.
[16] J.-P. Cohen-Addad, M. Domard, J. Herz, NMR observation of the swelling process of polydimethylsiloxane networks. Average orientational order of monomeric units, J. Chem. Phys. 76 (1982) 2744–2753.
[17] J. Kelm, K. Tobisch, J. Leisen, Comparative investigations of the cross-link density of elastomers, Kautsch. Gummi Kunstst. 51 (1998) 364–369.